SEISMIC WAVEFORMS AT ENGINEERING BEDROCKS BENEATH LIFELINES SUFFERED BY LIQUEFACTION IN THE 2011 OFF THE PACIFIC COAST OF TOHOKU EARTHQUAKE

M. Hara(1), G. Shoji(2), R. Terajima(3)

(1) Graduate Student, Department of Engineering Mechanics and Energy, University of Tsukuba, s1620916@u.tsukuba.ac.jp
(2) Associate Professor, Faculty of Engineering, Information and Systems, University of Tsukuba, gshoji@kz.tsukuba.ac.jp
(3) Mitsui & Co., Ltd., Former Graduate Student, Department of Engineering Mechanics and Energy, University of Tsukuba

Abstract

In the 2011 off the Pacific coast of Tohoku earthquake (hereinafter the Tohoku earthquake), buried pipes for water supply, water treatments and telecommunication networks were severely damaged due to severe ground motions and induced liquefaction. Physical damage of buried pipes caused the functional disruption of associated lifeline facilities. In order to clarify the mechanism of the damage by combined actions of severe ground motions and liquefactions, first, we performed series of analyses on the seismic wave propagation in the Tohoku and Kanto areas in the Tohoku earthquake and revealed the trends of seismic waveforms in the affected regions by severe liquefaction: Hitachinaka City and Kamisu City in Ibaraki Prefecture, and Mihama in Chiba City. The synthetic waveforms at engineering bedrocks were computed using the finite difference method with fourth-order spatial and second-order temporal discretization proposed by Aoi and Fujiwara (1999) Second, we focused onto the occurrence of liquefaction at two sites: an inherently liquefiable site (HOR2) and relatively non-liquefiable site (HOR1) in Kamisu City, in which the affected sewer pipes are distributed, based on effective stress analyses using one synthetic waveform and three observed waveforms near the associated liquefied areas in the Tohoku earthquake.

For the HOR2 site subjected to the synthetic waveform which wave amplitude at the engineering bedrock shows more than 0.5 m/s and 1.0 m/s^2 with the abundance of about 3.0 s long-period components, but that is a relatively smaller amplitude level, the excess pore water pressure ratio gradually increases to the liquefaction criterion of 97% with the long duration of about 100 s excitation. In contrast, for the HOR1 site subjected to observed waveforms with the less long-period components but long duration of more than 100 s showing a relatively larger intensity of about 4.0 m/s^2 after the main shocks, the excess pore water pressure ratio also reaches gradually and exceed the liquefaction level. Therefore, the input acceleration to the engineering bedrock with the rich long-period component of more than about 3.0 s and the long duration of more than about 100 s could gradually induce the liquefaction for an inherently liquefiable ground surface such as the Kamisu HOR2 site. From the other aspect, the input acceleration with the long duration of about 100 s after the main shocks showing the maximum intensity of about 4.0 m/s^2 also could induce the liquefaction for a relatively non-liquefiable ground surface such as the Kamisu HOR1 site.

Keywords: the 2011 off the Pacific coast of Tohoku earthquake, sewer pipes, liquefaction, effective stress analysis

1. Introduction

Buried pipes for water supply systems, water treatments and telecommunication networks were severely damaged in the 2011 off the Pacific coast of Tohoku earthquake (hereinafter the Tohoku earthquake). The damages were caused by combined actions of extreme ground motions and liquefaction. We need to analyze statistically the damage data and formulate the damage function as a measure for predicting the risks of buried-pipe damage in the huge earthquakes such as the anticipated Nankai trough earthquake. As previous studies on damage analysis of buried pipes in the Tohoku earthquake, for example, Tsukiji and Shoji (2013) [1] clarified the damage of distribution pipes of water supply systems at Itako City and Kamisu City in Ibaraki Prefecture where were liquefied severely, in terms of detailed topographical classification, ground condition, pipe type and pipe diameter. Shoji *et al.* (2014) [2] clarified the damage of sewer pipes at Hitachinaka City and Kamisu City in Ibaraki Prefecture and Mihama in Chiba City. They also developed the associated damage functions. However, these results cannot explain the physical mechanism of damage of buried pipes by considering mechanical underground characteristics such as ground water level, permeability property and thickness of liquefied layer and non-liquefied layer.

From the reasons above, first, we perform series of analyses about the seismic wave propagation in the Tohoku and Kanto areas in the Tohoku earthquake by the finite difference method with fourth-order spatial and second-order discretization by Aoi and Fujiwara (1999) [3], and reveal the trends of seismic waveforms at engineering bedrocks beneath the sewer pipes in the affected areas by severe liquefaction: Hitachinaka City and Kamisu City in Ibaraki Prefecture and Mihama in Chiba City as shown in Fig. 1. Second, we carry out one-dimensional (1D) seismic response analysis for the ground surfaces at two sites: an inherently liquefiable site (HOR2) and relatively non-liquefiable site (HOR1) in Kamisu City based on effective stress method by YUSAYUSA-2 [4] with the synthetic waveform by above finite difference method and three observed waveforms at Kamisu City and Chiba City. Hence, we clarify the amplification characteristics of ground shakings at liquefied and non-liquefied layers and the temporal transient process of liquefaction for subject ground surfaces.

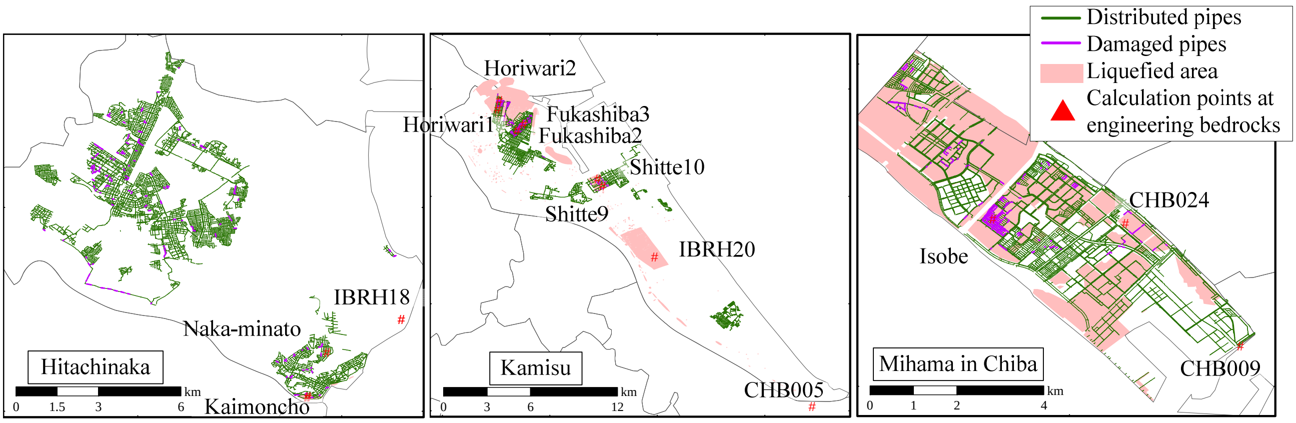

Fig. 1 – The subject areas for analysis

2. Input ground motions and underground modeling

2.1 Input wave setting

In one-dimentional seismic response analysis for the ground surfaces at two sites: HOR1 and HOR2, where buried sewer pipes were distributed, we use the synthetic waveform at engineers bedrocks beneath subject areas as an input waveform named for IW I as the velocity time series and the Fourier amplitude are shown in Fig. 2. Basically the associated synthetic waveforms at engineering bedrocks in the Tohoku and Kanto area were computed using the finite difference method with fourth-order spatial and second-order temporal discretization proposed by Aoi and Fujiwara (1999) [3]. We used the fault source model estimated by Yagi and Fukahata (2011) [5] which is 200km width and 500km length and consists of 25 × 10 subfaults which is 20×20 km^2. We adopted Japan Integrated Velocity Structure Model by the Headquarters for Earthquake Research Promotion [6] for setting the boundary depth and the physical characteristics of the underground structure. Fig. 3 and Fig. 4 show that the analytical region and the grids for the computation. As shown in Fig. 4, the region 1, in which the grid size is set to be smaller, is suitable for the complex surface layers and the region 2, in which the grid size is set to be larger, is suitable for the deeper underground structure. The grid size in region 2 was set to be 3 times as large as that in region 1. We set the boundary between region 1 and 2 to be 8 km depth following the shear velocity V_s of about 3 km/s. Table 1 shows the overview of numerical conditions.

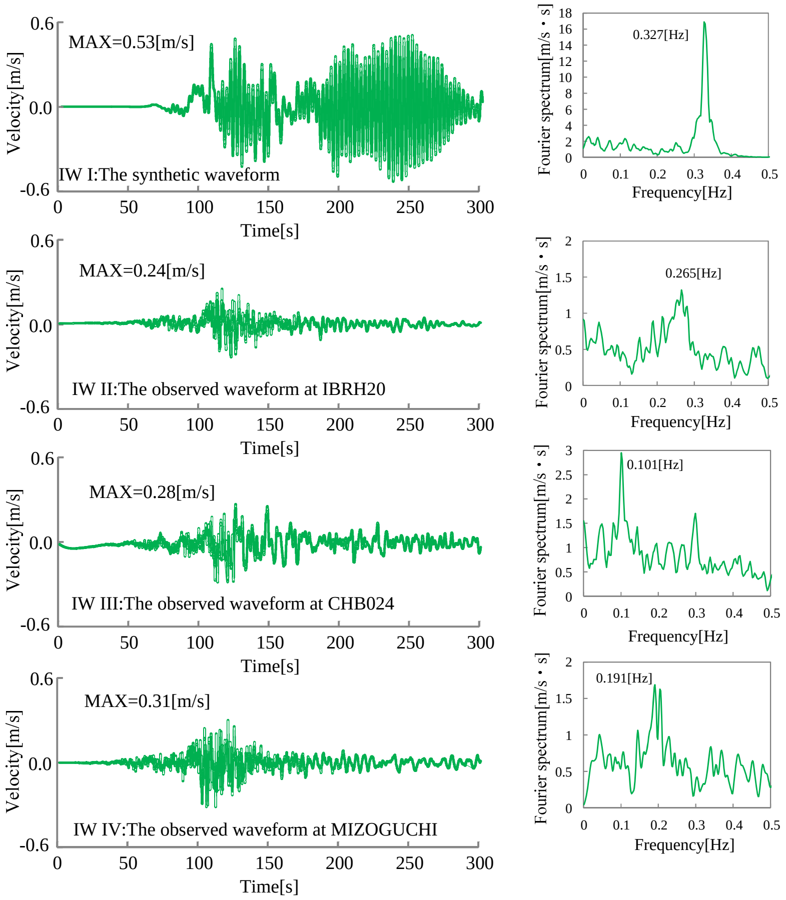

Fig. 2 – Input waveforms

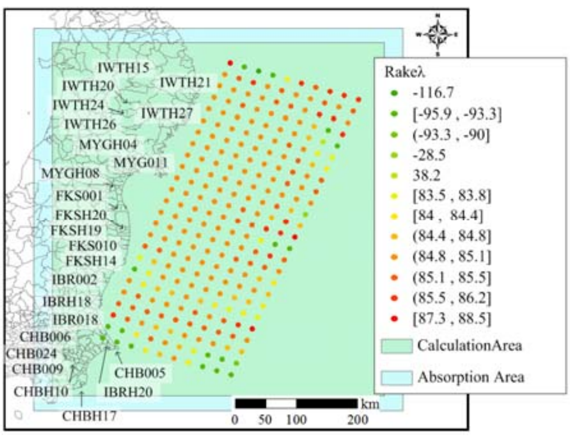

Fig. 3 – Computational region and source model

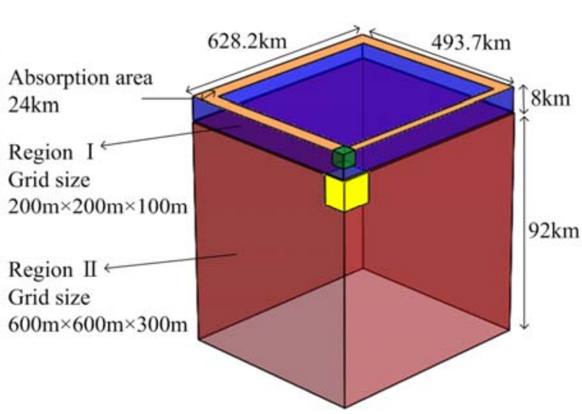

Fig. 4 – Grids for computation

Table 1 – Numerical conditions

	RegionI	RegionII
Maximum frequency	0.5Hz	
Sampling number	60000	
Sampling period	0.005s	
Duration	300s	
Horizontal grid size	200m	600m
Vertical grid size	100m	300m
Discontinuous boudary	8km	
Grid number in absorption area	120	40
Attenuation constant of absorption area	0.0025	0.0075

In addition to IW I waveform, we use three observed waveforms, named for IW II to IW IV as shown in Fig. 2. IW II was observed at IBRH20 by KiK-net which is located near the liquefied area in Kamisu City. It contains the predominant period of about 3.8 s, which shows slightly longer than that of IW I. IW III was observed at CHB004 by K-NET which is located in severely and typically liquefied area at Mihama in Chiba City. It has two predominant periods of more than 10 s and about 3.3 s. IW IV was captured in the local government office at Mizoguchi in Kamisu City. Near the sites at Shitte we can also observed the damage of sewer pipes due to the liquefaction. It has the longer predominant period of about 5.2 s compared with IW I, II and III.

2.2 Underground model

Two sites in Kamisu City : HOR1 and HOR2 are selected for analysis because these two sites were liquefied in the Tohoku earthquake and Kamisu City investigated enough information about the soil profiles for the restoration of the sites and the countermeasures to liquefaction. Liquefaction at HOR2 site occurred more severely than that at HOR1 site. Fig. 5 shows the geological columnar sections and the results of standard penetration tests at two sites. At HOR2 site, the ground water level is 1.4 m depth and there is some possibility of occurrence of liquefaction at the 2nd layer which consists of dredget soil. In contrast, at HOR1 site, the ground water level is 0.8m depth which is shaller one than that at HOR2 and the 2nd layer consisting of filling soil might be liquefied.

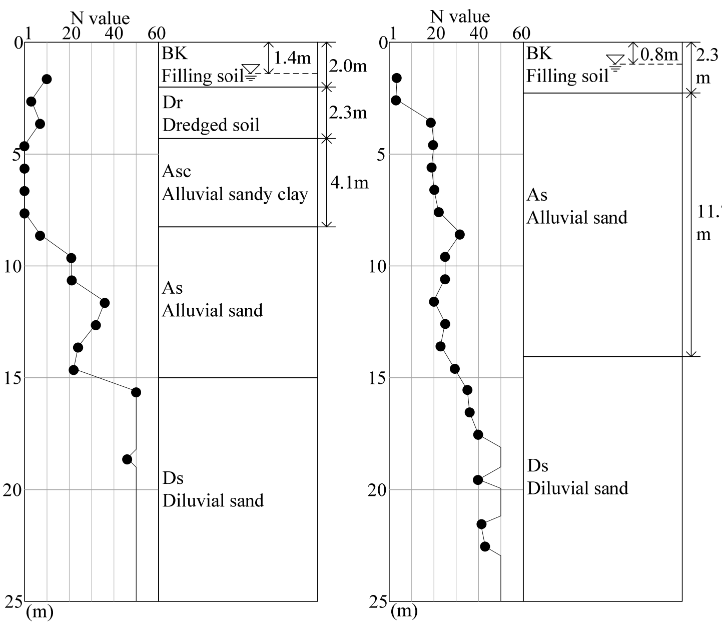

Fig. 5 – Soil profiles at HOR2 and HOR1

Table 1 shows the physical propties for ground surfaces at the two sites. The parameters in the models were determined by the associated soil tests. We estimated the information about the layers which is not obtained directly by the tests by using the liquefaction strength R and the internal friction angle ϕ based on the method by Japan Road Association [7] and the formulations by Hatanaka and Uchida (1996) [8] respectively. We also estimated the coefficient of permeability k and the Creager's coefficient [9] respectively. We used the same parameters at HOR2 site as ones at HOR1 site under 8.25m depth due to luck of the results of the soil tests. We assumed that the valued of 97% is limit of the excess pore water pressure ratio and criterion of liquefaction.

Table 1– Physical proparties

(a) At HOR2 site

No.	Top surface depth [m]	Layer thickness [m]	Wet density ρ_t[kN/m^3]	Porosity n	Coefficient of permeability k[m/s]	Coefficient of volume compressibility m_v[m^2/kN]	Initial modulus of rigidity G_0[kN/m^2]	Shear stress τ_f[kN/m^2]
1	0	1.4	17.856	0.461	4.2×10^{-5}	8.92×10^{-6}	38790	22.2
2	1.4	2.6	17.856	0.461	4.2×10^{-5}	6.94×10^{-6}	38790	22.2
3	4	2	16.817	0.565	4.0×10^{-8}	6.48×10^{-6}	24660	22.7
4	6	2.25	16.817	0.565	3.3×10^{-6}	5.90×10^{-6}	24660	22.7
5	8.25	3	18.924	0.434	4.8×10^{-5}	4.96×10^{-6}	68180	51.2
6	11.25	3.75	18.924	0.434	4.4×10^{-5}	4.49×10^{-6}	68180	51.2
7	15	3.5	18.355	0.434	4.4×10^{-5}	4.17×10^{-6}	68180	51.2
8	18.5	3.5	18.355	0.430	1.2×10^{-4}	3.92×10^{-6}	102540	117
9	22	3.4	18.355	0.430	1.2×10^{-4}	3.73×10^{-6}	102540	117

(b) At HOR1 site

No.	Top surface depth [m]	Layer thickness [m]	Wet density ρ_t[kN/m^3]	Porosity n	Coefficient of permeability k[m/s]	Coefficient of volume compressibility m_v[m^2/kN]	Initial modulus of rigidity G_0[kN/m^2]	Shear stress τ_f[kN/m^2]
1	0	0.8	18.13	0.453	3.5×10^{-5}	1.10×10^{-5}	58990	29.8
2	0.8	1.5	18.13	0.453	3.5×10^{-5}	8.54×10^{-6}	58990	29.8
3	2.3	2.5	18.248	0.447	3.3×10^{-5}	6.81×10^{-6}	70530	24.7
4	4.8	1.2	18.248	0.447	4.0×10^{-5}	6.33×10^{-6}	70530	24.7
5	6	2.25	18.248	0.447	2.6×10^{-5}	5.52×10^{-6}	70530	24.7
6	8.25	3	18.924	0.434	4.8×10^{-5}	4.96×10^{-6}	68180	51.2
7	11.25	3.75	18.924	0.434	4.4×10^{-5}	4.49×10^{-6}	68180	51.2
8	15	3.5	18.355	0.434	4.4×10^{-5}	4.17×10^{-6}	68180	51.2
9	18.5	3.5	18.355	0.430	1.2×10^{-4}	3.92×10^{-6}	102540	117
10	22	3.4	18.355	0.430	1.2×10^{-4}	3.73×10^{-6}	102540	117

3. Relation between input waveforms and liquefaction transient process

3.1 Liquefaction process at HOR2 site

Fig. 6(a)-(d) show the input acceleration and the acceleration, the displacement, the excess pore water pressure ratio and the effective stress pass in the 2nd layer of dredged soil at HOR2 site.

For the case of IW I (Fig. 6 (a))The excess pore water pressure ratio starts to increase sharply at 110 s and 190 s with the corresponding increase of the acceleration amplitude, and reaches 97% at 250 s. The peak amplitude of acceleration in the 2nd layer is 1.28 times as large as one in base layer. The displacement amplitude increases rapidly after peaks of the excess pore water pressure ratio and reaches the maximum value of 0.12 m.

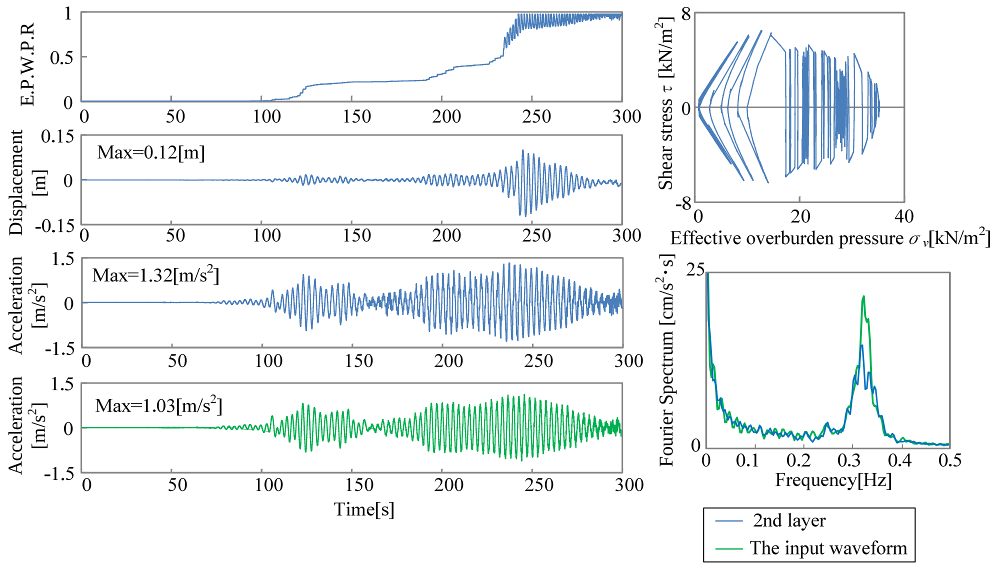

Fig. 6(a) – The results at HOR2 for the case of IW I

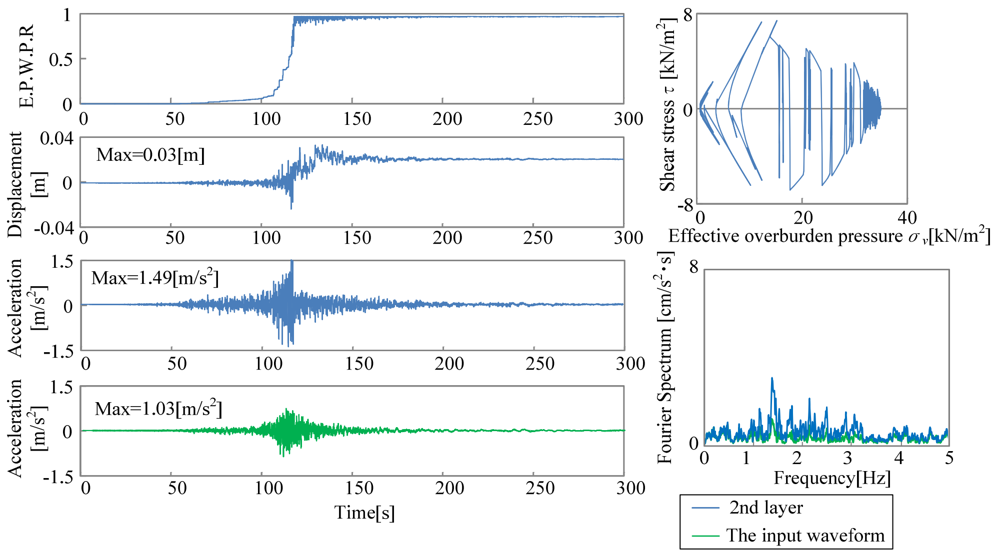

Fig. 6(b) – The results at HOR2 for the case of IW II

For the case of IW II (Fig. 6 (b)), the 2nd layer is also liquefied. The pore water pressure ratio starts to increase more sharply at about 105 s than that for the case of IW I and reaches the liquefaction criterion after peaks of acceleration amplitude at 119 s. In contrast the amplitude of acceleration decreases rapidly after the occurrence of liquefaction. The peak acceleration at the 2nd layer is as twice as the peak acceleration of input waveform.

For the case of IW III (Fig. 6 (c)), the excess pore water pressure ratio increases to 40 % in the time series from 40 s to 70 s. It increases again from 50% to 97% at about 80 s when relatively large acceleration amplitude occurs after the main shock. Although the peak acceleration of the input waveform for the case of IW III shows more than four times larger than that for the case of IW II, the peak accelerations at the 2nd layer for IW II and III cases show almost same amplitudes of 1.49 m/s^2 and 1.44 m/s^2. In addition the peak displacement in the 2nd layer shows maximum of 0.36 m among four cases.

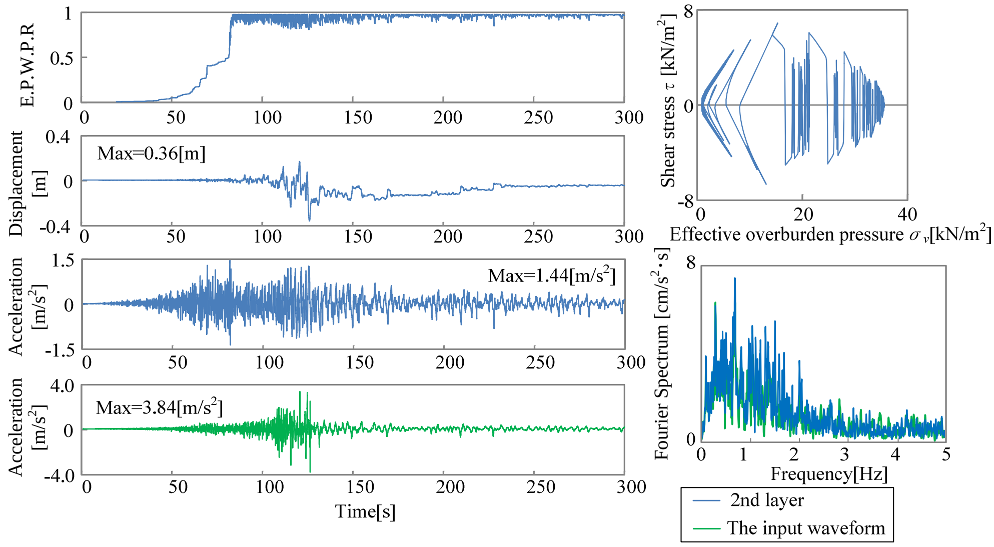

Fig. 6(c) – The results at HOR2 for the case of IW III

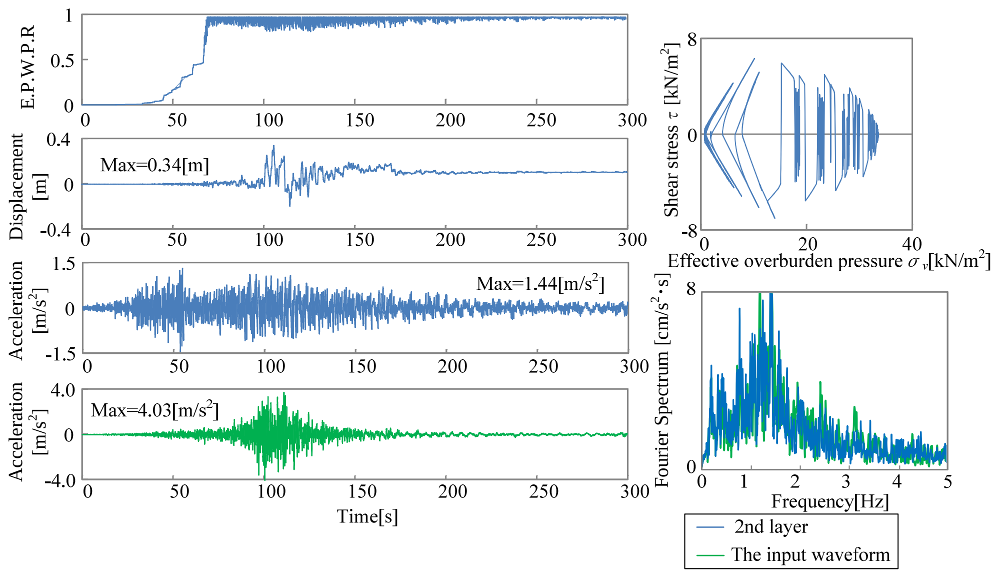

Fig. 6(d) – The results at HOR2 for the case of IW IV

For the case of IW IV (Fig. 6 (d)), the transient process of the excess pore water pressure shows the similar trend to that for the case of IW III. The peak amplitude of the input acceleration for the case of IW IV shows slightly larger than that for the case of IW III, however the peak accelerations at the 2nd layer for both cases show almost same. The reason is why the peak acceleration response at the 2nd layer has the limit and saturates around about 1.4 m/s^2 during the liquefaction for the HOR2 soil profile. The peak displacement at the 2nd layer for the case of IW IV becomes almost same value of 0.34 m as that for the case of IW III.

3.2 Liquefaction process at HOR1 site compared with that at HOR2 site

Fig. 7(a)-(d) show the input acceleration and the acceleration, the displacement, the excess pore water pressure ratio and the effective stress pass in the 2nd layer of filling soil, BK at HOR1 site.

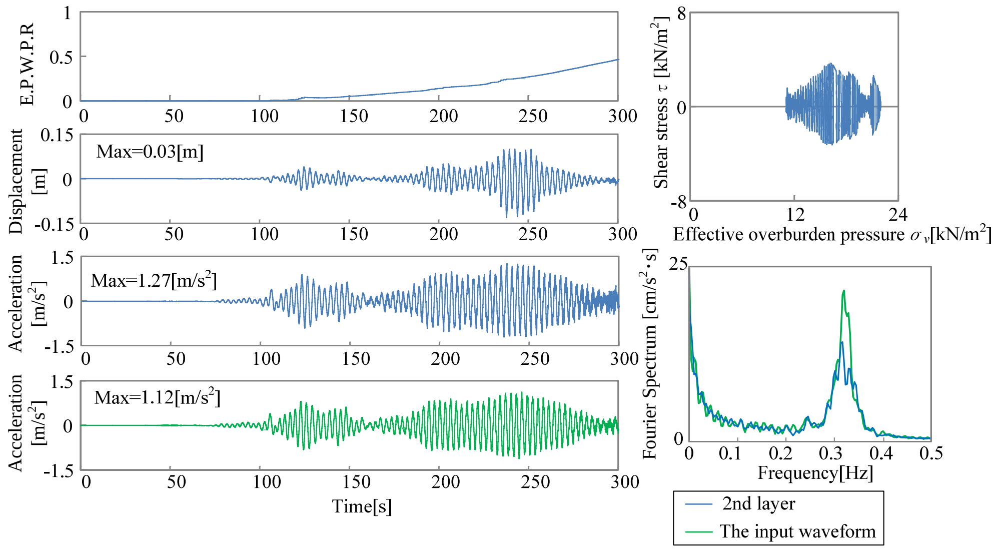

Fig. 7(a) – The results at HOR1 for the case of IW I

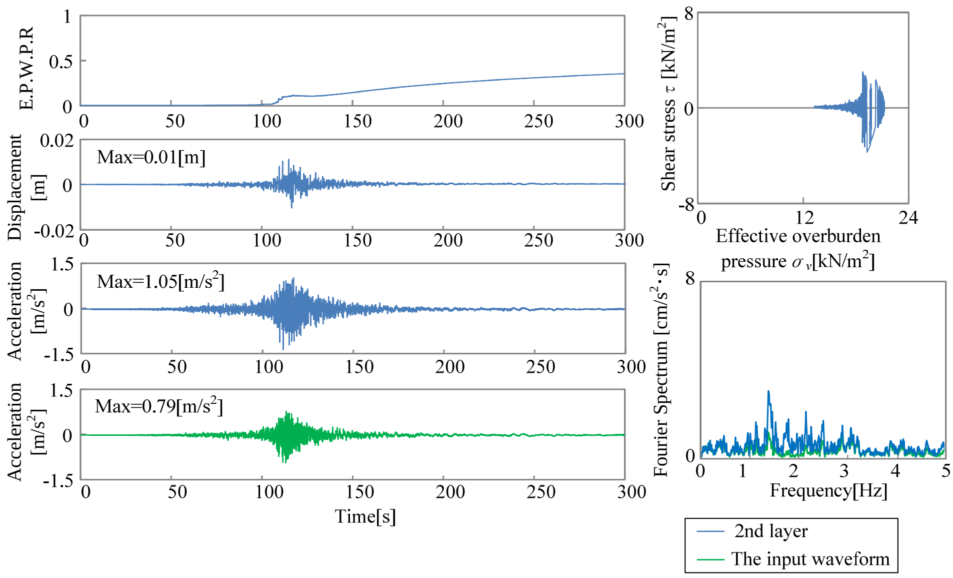

Fig. 7(b) – The results at HOR1 for the case of IW II

For the case of IW I (Fig. 7 (a)),, the excess pore water pressure ratio at HOR1 site increases more gradually from about 120 s to 300 s than that at HOR2 site and reaches 46% even at 300 s which means HOR1 site is not liquefied subjected to the IW I input waveform. The displacement response becomes considerably smaller than that at HOR2 site. The seismic responses at the 2nd layer for the case of IW II (Fig. 7 (b)) do not show the liquefaction as well as those for the case of IW I. In contrast, for the cases of IW III (Fig. 7 (c)) and IW IV (Fig. 7 (d)), the excess pore water pressure ratio starts to increase immediately after about 50 s with increasing of the acceleration amplitude of the input waveform, and reaches the liquefaction criterion at 224 s and 172 s after the long duration of more than 170 s and 120 s compared with that at HOR2 site subjected to IW III and IV. Long-period wave excitation after about 130 s strongly induces the liquefaction process for the HOR1 soil profile. In addition the peak displacements show same value of 0.20 m and the residual displacements occur in both cases of IW III and IV although the two time series about displacement have the different trends.

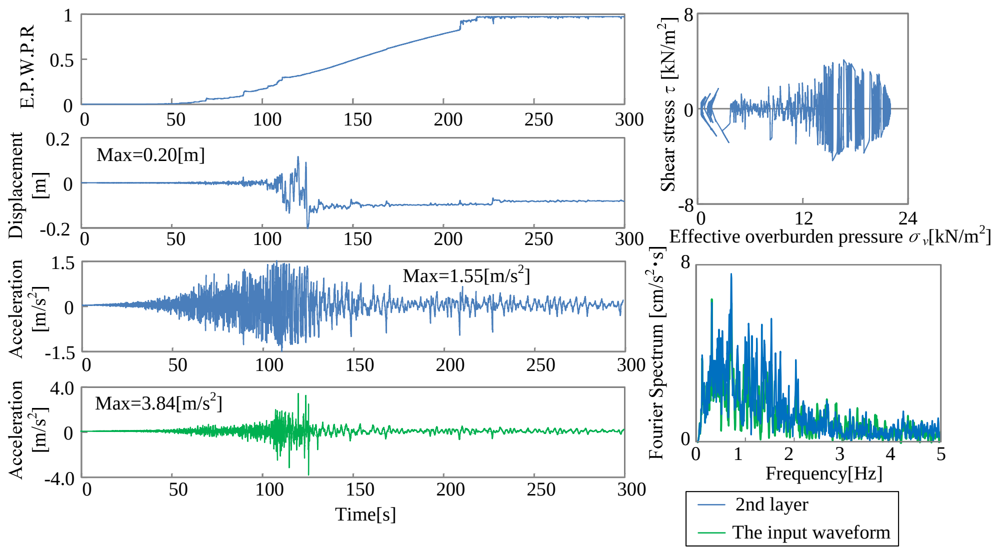

Fig. 7(c) – The results at HOR1 for the case of IW III

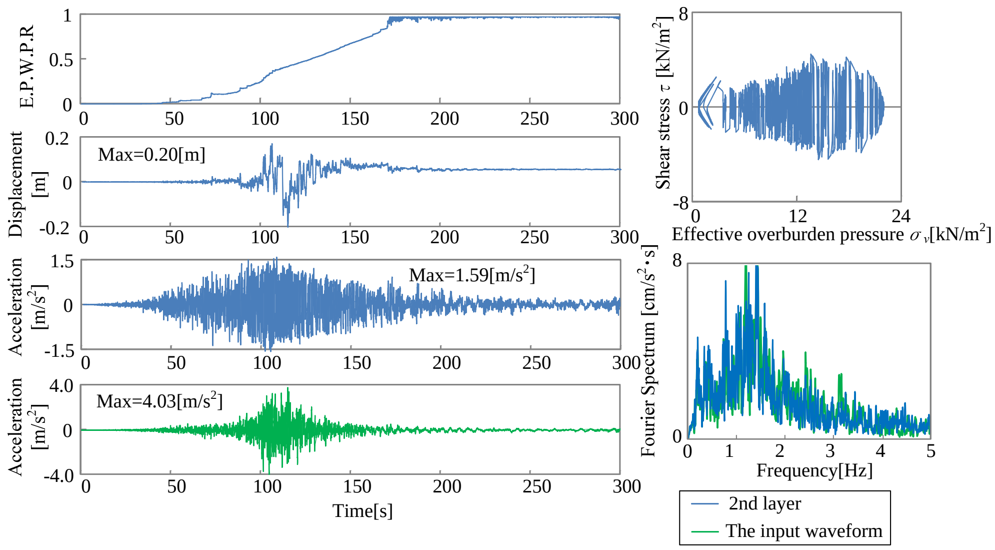

Fig. 7(d) – The results at HOR1 for the case of IW IV

By comparing the liquefaction transient processes subjected to the IW I, II, III and IV input waveforms at HOR2 and HOR1 sites, the input acceleration to the engineering bedrock with the long-period component of more than about 3.0 s and the long duration of more than about 100 s such as IW I could gradually induce the liquefaction for an inherently liquefiable ground surface such as the HOR2 site. In addition, the input acceleration with the long duration of about 100 s after the main shocks showing the maximum intensity of about 4.0 m/s^2 such as IW III and IV also could induce the liquefaction for a relatively non-liquefiable ground surface such as the HOR1 site.

4. Conclusion

In order to clarify the mechanism of the damage by combined actions of severe ground motions and liquefactions, first, we performed series of finite difference numerical simulation on the seismic wave propagation in the Tohoku and Kanto areas in the Tohoku earthquake and revealed the trends of seismic waveforms in the affected regions by severe liquefaction: Hitachinaka City and Kamisu City in Ibaraki Prefecture, and Mihama in Chiba City. Second, we focused onto the occurrence of liquefaction at two sites: an inherently liquefiable site (HOR2) and relatively non-liquefiable site (HOR1) in Kamisu City, in which the affected sewer pipes are distributed, based on effective stress analyses using one synthetic waveform and three observed waveforms near the associated liquefied areas in the Tohoku earthquake. The following results were concluded.

For the HOR2 site subjected to the synthetic waveform which wave amplitude at the engineering bedrock shows more than 0.5 m/s and 1.0 m/s^2 with the abundance of about 3.0 s long-period components, but that is a relatively smaller maximum amplitude level, the excess pore water pressure ratio gradually increases to the liquefaction criterion of 97% with the long duration of about 100 s excitation. In contrast, for the HOR1 site subjected to observed waveforms with the less long-period components but long duration of more than 100 s showing a relatively larger intensity of about 4.0 m/s^2 after the main shocks, the excess pore water pressure ratio also reaches gradually and exceed the liquefaction level.

Therefore, the input acceleration to the engineering bedrock with the rich long-period component of more than about 3.0 s and the long duration of more than about 100 s could gradually induce the liquefaction for an inherently liquefiable ground surface such as the Kamisu HOR2 site. From the other aspect, the input acceleration with the long duration of about 100 s after the main shocks showing the maximum intensity of about 4.0 m/s^2 also could induce the liquefaction for a relatively non-liquefiable ground surface such as the Kamisu HOR1 site.

5. Acknowledgements

We appreciate valuable cooperation for related local government sectors in Kamisu City and committees for countermeasures of liquefaction damages in Kamisu City. This study was sponsored by the integrated risk management project for complex disasters on large-scale earthquakes at University of Tsukuba (leader, Professor Y. Yagi). Finally, we also have the financial support and sustainable encouragement from Professor N. Nojima of Gifu University, Dr. S.Nagata of Kajima Technical Research Institute and Associate Professor Y. Maruyama of Chiba University.

6. References

[1] Tsukiji T, Shoji G (2013): Development of damage functions on water supply systems subjected to an extreme ground motion, Proceedings of the 11th International Conference on Structural Safety and Reliability (ICOSSAR2013), New York, USA, *Safety, Reliability, Risk and Life-Cycle Performance of Structures & Infrastructures* eds by G. Deodatis, B. R. Ellingwood and D. M. Frangopol, CRC Press Taylor & Francis Group, London, ISBN 978-1-138-00086-5, 691-698.

[2] Shoji G, Terajima R, Nagata S (2014): Development of damage functions on sewer buried pipelines subjected to an extreme ground motion from damage assessment based on the data in recent earthquakes, *Journal of Japan Society of Civil Engineers,* Ser. A1 (Structural Engineering & Earthquake Engineering (SE/EE)), **70**(4), I_921-I_946.

[3] Aoi S, Fujiwara H (1999): 3-D finite difference method using discontinuous grids, *Bulletin of the Seismological Society of America*, **89**, 918-930.

[4] Yoshida N: YUSAYUSA-2, http://www.civil.tohoku-gakuin.ac.jp/yoshida/computercodes/index.html (2016/4/23)

[5] Yagi Y, Fukahata Y (2011): Rupture process of the 2011 Tohoku-oki earthquake and absolute elastic strain release, *Geophysical Research Letters*, **38**, doi:10.1029/2011GL048701.

[6] The Headquarters for Earthquake Research Promotion, http://www.jishin.go.jp/main/chousa/12_choshuki/dat/ (2016/4/23)

[7] Japan Road Association (2002): Design Specifications of Highway Bridges, Part V Seismic Design.

[8] Hatanaka M, Uchida A (1996): Empirical correlation between penetration resistance and internal friction angle for sandy soils, *Soils and Foundations*, **36**(4), 1-9.

[9] Creager WP, Justin JD, Hinds J (1945): *Engineering for Dams*, Vol. III, Earth, Rock-fill, Steel and Timber dams, John Wiley & Sons, Inc., N.Y., 645-649.